

Fast Subject-Specific Local SAR and B_1^+ Prediction for PTx at 7T using only an Initial Localizer Scan

Wyger Brink¹, Marius Staring², Rob Remis³, and Andrew Webb¹

¹C.J. Gorter Center for High Field MRI, dept. of Radiology, Leiden University Medical Center, Leiden, Netherlands, ²Division of Image Processing, dept. of Radiology, Leiden University Medical Center, Leiden, Netherlands, ³Circuits and Systems group, dept. of Microelectronics, Delft University of Technology, Delft, Netherlands

Synopsis

This work presents a method for local SAR and B_1^+ prediction using only a 9 seconds long localizer as an input. The total procedure can be executed in less than 30 seconds for a birdcage configuration and less than 45 seconds for a PTx configuration, which enables seamless integration into the MR workflow.

Introduction

Ultra-high field (UHF) MRI ($B_0 > 7T$) shows great promise to yield higher resolution structural and physiological information than available at 3T, particularly in the brain. Parallel RF transmission (PTx) is a key technology for UHF-MRI to address the increased spatial variations in the radiofrequency (RF) field distribution. However, currently it has failed to reach widespread clinical adoption. The main factors include the intersubject variability in local specific absorption rate (SAR) leading to large safety margins to ensure compliance to regulatory limits^{1,2}, and time-consuming B_1^+ calibration procedures required for tailored RF pulse design. Together, these technological challenges limit the clinical impact of PTx and the utilization of UHF-MRI.

In this work, we demonstrate a fast subject-specific method based on deep learning and a fast EM solver for predicting both local SAR and B_1^+ fields using only a 9 second long localizer scan. A schematic overview of the approach is shown in Figure 1.

Methods

MR protocol: Data was acquired in 20 healthy volunteers (10 male, 10 female, age range 21-66 years) on a Philips Achieva 7T MRI system equipped with a Nova Medical birdcage head coil and integrated 32-channel receive coil array. The imaging protocol consisted of a 3D T_1 -weighted MP-RAGE sequence acquired at 1 mm isotropic resolution in 3 min, followed by a fast 3D T_1 -weighted localizer acquired at 2 mm isotropic resolution in 9 s.

The 1 mm T_1 -weighted data were first used to generate subject-specific dielectric body models with eight tissue classes using our recently developed deep learning segmentation method³. The resulting material parameter maps (i.e. permittivity, conductivity, density) were subsequently downsampled to 2 mm and used as 'ground truth' data for training the deep learning network with the localizer as input.

Deep Learning: A 2.5D convolutional neural network was implemented based on the ForkNET topology⁴. The network was designed to have one input and 5 outputs, consisting of the three tissue parameters and additional masks for the background and internal air. The network was implemented using TensorFlow and trained in 100 epochs using a mean squared error loss function. To ensure generalizability, the results were tested in a leave-one-out manner, in which the test subject was excluded from the training data.

EM Solver: The B_1^+ field and 10 g-averaged SAR distribution (SAR_{10g}) in the ground truth and localizer-based body models were simulated using a previously developed custom EM solver based on the volume integral equation method⁵. The solver employs a numerical Green's tensor computed via FDTD and includes a pre-computed coil response library to account for the loading of the RF coil. Incident fields for a quadrature birdcage as well as a generic PTx loop array were simulated using FDTD (XF7.4, Remcom inc., State College, PA) and the solver was implemented in Matlab (2021a, Mathworks inc., Natick, MA) facilitating parallel computing and GPU acceleration through an Nvidia K40 GPU. Channelwise E-fields were combined to construct Q-matrices, averaged over 10 g and processed into a SAR oracle format to facilitate efficient SAR evaluation^{6,7}.

Results

Training of the deep learning network took approximately 160 min and final inference took approximately 1s per subject. A comparison between ground truth and localizer-based dielectric body models is shown in Figure 2.

Figure 3 shows a convergence analysis of the EM solver with respect to discretization step size, evaluated in the birdcage configuration. The peak local SAR error drops below ~1% on average for spatial resolutions of 4.0 mm and higher, which strikes an appropriate balance with an average computation time of 12s. In the eight-channel PTx configuration, the average computation time was 32s, including parallel computing overhead.

Quadrature birdcage simulations in five of the ground truth and localizer-based body models are shown in Figure 4. Overall, peak SAR_{10g} values obtained in the network generated body models are within 5% of those obtained in the ground truth body models.

Peak SAR_{10g} predictions in 1000 random PTx excitations were evaluated against those obtained in the corresponding ground truth body models, summarized in Figure 5. The average peak SAR_{10g} overestimation in the localizer-based models was 2.2% and an additional 6.3% safety margin would be required to ensure a conservative local SAR estimate in 95% of the cases. This is a considerable improvement compared to the average overestimation of 45.2% that would be obtained by assuming worst-case local SAR values.

Discussion/Conclusion

This work presents a method for local SAR and B_1^+ prediction using only a short localizer as an input. The total procedure can be executed in less than 30 seconds for the birdcage configuration and less than 45 seconds for the PTx configuration, which enables seamless integration into the MR workflow. As a localizer is acquired at the start of any MR protocol, and the resulting B_1^+ information can replace time-consuming B_1^+ calibration procedures, the method does not place a time burden on the MR examination. The SAR predictions can be used to personalize the safety margins, design SAR-optimized RF pulses to safely increase the headroom in allowed sequence parameters.

Acknowledgements

The authors thank Dr. Chloé Najac and Kevin Keene for assistance in data acquisition. This work was supported by the Nederlandse Organisatie voor Wetenschappelijk Onderzoek (NWO) through a VENI fellowship (TTW.16820).

References

1. le Garrec M, Gras V, Hang MF, Ferrand G, Luong M, Boulant N. Probabilistic analysis of the specific absorption rate intersubject variability safety factor in parallel transmission MRI. *Magnetic Resonance in Medicine* 2017;78:1217–1223 doi: 10.1002/mrm.26468.
2. Ajanovic A, Hajnal J v, Malik S. Positional Sensitivity of Specific Absorption Rate in Head at 7T. In: *Proceedings of the 28th Annual Meeting of ISMRM, Virtual Conference.* ; 2020. p. 4251.
3. Brink W, Yousefi S, Bhatnagar P, Staring M, Remis R, Webb A. Numerical Body Model Inference for Personalized RF Exposure Prediction in Neuroimaging at 7T. In: *Proceedings of the 29th Annual Meeting of the ISMRM, Virtual Meeting.* ; 2021.
4. Rashed EA, Diao Y, Hirata A. Learning-based estimation of dielectric properties and tissue density in head models for personalized radio-frequency dosimetry. *Physics in medicine and biology* 2020;65 doi: 10.1088/1361-6560/AB7308.
5. Brink WM, van Gemert JHF, Remis RF, Webb AG. Accelerated SAR Computations by Exploiting Sparsity in the Anatomical Domain. In: *Proceedings of the 27th Annual Meeting of ISMRM, Montreal.* ; 2019. p. 0735.
6. Kuehne A, Seifert F, Ittermann B. GPU-Accelerated SAR Computation with Arbitrary Averaging Shapes. In: *Proceedings of the 20th Annual Meeting of ISMRM, Melbourne, Australia.* ; 2012. p. 2735.
7. Pendse M, Stara R, Khalighi MM, Rutt B. IMPULSE: A scalable algorithm for design of minimum specific absorption rate parallel transmit RF pulses. *Magnetic Resonance in Medicine* 2019;81:2808–2822 doi: 10.1002/MRM.27589.

Figures

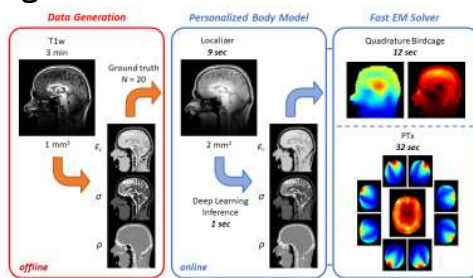


Fig. 1. Schematic overview of the approach. Ground truth dielectric body models ($N=20$) were generated from T_1 -weighted datasets acquired at 1 mm^3 resolution. The deep learning method was then trained using the corresponding 9s localizer data acquired at 2 mm^3 resolution as input. Local SAR and B_1^+ fields are finally simulated using a custom EM solver.

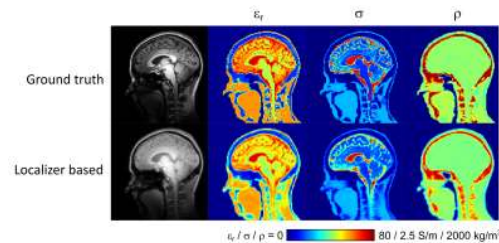


Fig. 2. Example of a subject-specific dielectric body model derived from the 9s localizer compared to the ground truth. Shown are sagittal cross sections of the T_1 -weighted and localizer data, and corresponding material property maps.

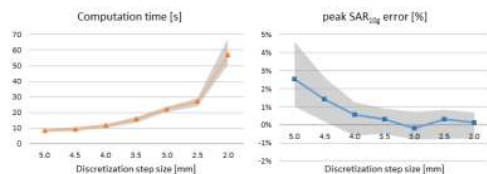


Fig. 3. Numerical convergence analysis of the EM solver evaluated in the birdcage configuration ($N=5$). Shown are the average computation time and average peak SAR_{10g} error relative to results obtained at 1.5 mm . Grey bands indicate min/max ranges.

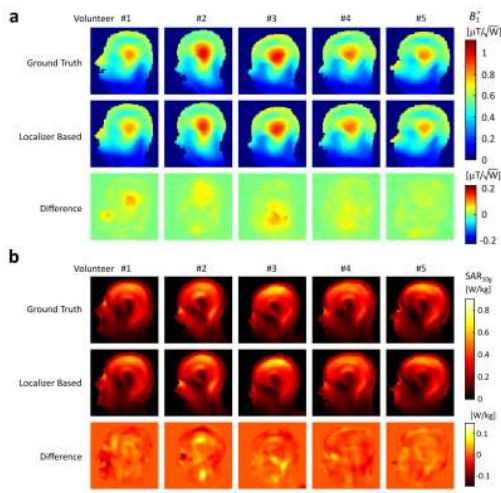


Fig. 4. B_1^+ (a) and SAR_{10g} (b) simulations in the quadrature birdcage configuration, comparing predictions obtained in the ground truth body models against those obtained in localizer-based body models.

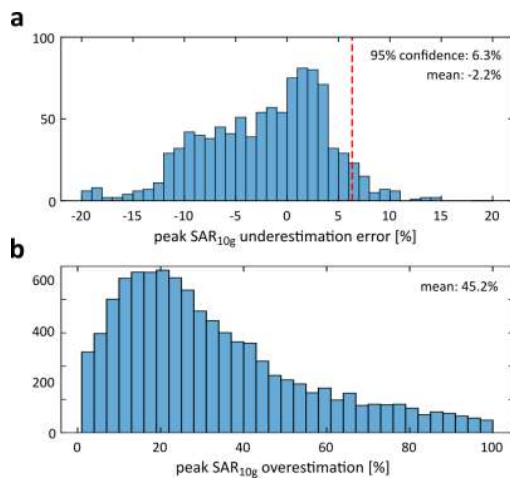


Fig. 5. PTx peak SAR_{10g} predictions evaluated in 1000 random excitations, showing prediction errors in the personalized approach (a) and overestimations when assuming worst case values (b). The data indicate that the localizer-based approach results in an effective safety margin of 8.5% to ensure conservative SAR estimation in 95% of the cases. This is a considerable improvement compared to the average overestimation of 45.2% in the 'worst case' approach.